An Efficient Onboard Quantization Strategy for Multi-Channel SAR Systems

Michele Martone, Michelangelo Villano, Marwan Younis, and Gerhard Krieger
Microwaves and Radar Institute, German Aerospace Center, Michele.Martone@dlr.de, Germany

Abstract

Multi-channel SAR systems allow high-resolution imaging of a wide swath and represent an attractive solution for present and next-generation SAR mission concepts. However, their operation requires the downlink of a huge amount of data: in addition to the intrinsic data requirement related to resolution and swath, in fact, a pulse repetition frequency (PRF) higher than the processed Doppler bandwidth is usually selected. A convenient data reduction strategy is therefore proposed, which exploits the correlation between samples by performing variable-bit quantization of the data after a block transformation of the multichannel SAR data, e.g., an FFT. Simulations show that this allows reducing the data volume while keeping the same performance at the cost of a modest onboard processing effort.

1 Introduction

For the design of conventional single-channel SAR systems, it is well known that the pulse repetition frequency (PRF) poses opposite constraints for the achievement of large swath widths and, at the same time, of fine azimuth resolutions. Indeed, if, for the former, low PRFs are required to allow sufficient temporal separation between subsequent pulses, the latter imposes the utilization of large Doppler bandwidth and, therefore, of high PRFs.
In the last decades, innovative techniques exploiting multiple receiver apertures mutually separated in the along-track and digital beamforming have been investigated and suggested to overcome such inherent limitations. By coherently combining the individual received signals, the ambiguous parts of the Doppler spectra can be opportunely suppressed, and high-resolution wide-swath imaging is achieved [1], [2], [3], [4], [5], [6], [7]. For such systems a straightforward signal reconstruction is obtained in the case of uniform azimuth sampling, i.e. if the following constraint on the PRF is fulfilled

$$\mathrm{PRF} = \frac{2v_{\mathrm{sat}}}{N \cdot dx}, \tag{1}$$

being v_{sat} the satellite velocity, *N* the number of receiving channels, and dx the azimuth separation between the sub-apertures (i.e. the azimuth antenna length can be expressed as $L_{\mathrm{az}} = N \cdot dx$). In general, signal reconstruction can be effectively performed also in case of non-uniform azimuth sampling [1]. As a result, the bandwidth of the combined signal is higher than the system PRF, i.e. a better azimuth resolution is achieved with respect to the corresponding single-channel SAR with the full antenna length L_{az} and operating at the same receive PRF. It is worth pointing out that, for multi-channel SAR systems, PRF higher than the ratio of the processed bandwidth and the number of apertures (PRF>PBW$/N$) is required to guarantee a sufficient target azimuth ambiguity to signal ratio (AASR), and this further increases the resulting data volume.
The price to pay for such a substantial performance improvement, besides an increased system complexity, is represented by an enlarged amount of data to be managed, which implies, from mission design, harder requirements in terms of onboard memory and downlink capacity. In this scenario, efficient data volume reduction represents an essential aspect, since the resulting data rate allowed for the digitization of the recorded radar signals affects both the amount of data to be stored and transmitted to the ground, and the quality of the resulting SAR products. Recently, a data-driven data reduction method for multi-channel SAR has been proposed in [8], which grounds on the adoption of the principal component decomposition in combination with the flexible dynamic block adaptive quantization (FDBAQ [9]) scheme at the cost of a larger onboard computational cost.
In the next section, a simple but effective method for efficient data volume reduction for multi-channel SAR is presented, which exploits the intrinsic correlation existing among the data samples. In particular, the multi-channel data are decomposed by means of an orthogonal transformation, and, jointly, an efficient selection of the quantization rates is applied to the transformed coefficients, which allows to optimize the resulting performance for the selected data rate. Then, in Section 3, simulations for a C-band single-platform multi-channel SAR are conducted, and the preliminary results prove the effectiveness of the proposed compression scheme. In Section 4 conclusions are drawn.

2 Data Reduction Strategy for Multi-Channel SAR

Let us consider a multi-channel SAR composed by *N* azimuth sub-apertures. In such a system, the samples received by the *N* azimuth channels can be modeled as partially correlated random variables. Such a correlation is

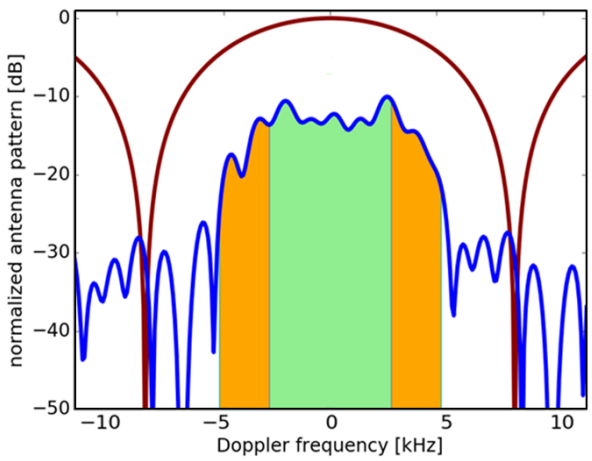

Figure 1: Two-way (blue) and single element receive patterns (dark red) versus Doppler frequency (in transmission a phase spoiled pattern is employed). The shaded green area indicates the processed bandwidth, whereas the $N \cdot \mathrm{PRF}$ effective sampling bandwidth is depicted in orange.

primarily due to a consistent oversampling of the azimuth data stream, and depends on the specific antenna pattern (or Doppler spectrum) and on the PRF [10]. Moreover, the effective PRF is typically larger than the actual processed bandwidth PBW

$$\mathrm{PRF}_{\mathrm{eff}} = N \cdot \mathrm{PRF}_{\mathrm{sys}} > \mathrm{PBW}. \tag{2}$$

Fig. 1 shows the single receiver element (in dark red) and the two-way antenna patterns (in blue) for a C-band multi-channel SAR with *N*=8 azimuth channels, which is considered in this study. Phase spoiling [11] is applied in transmission, and a system PRF ($\mathrm{PRF}_{\mathrm{sys}}$) of about 1170 Hz is considered. The actual processed bandwidth PBW is depicted in green and is about 5.6 kHz, which corresponds to 60% of the effective PRF ($8 \cdot 1170 \sim 9.4$ kHz). A list of the simulation parameters, considered for the present analysis, is given in Table 1. For such an exemplary system, it is worth pointing out that the relation in (1) is actually fulfilled, but, in general, a sophisticated calibration and reconstruction of the multi-channel signal needs to be implemented on ground. For this, several algorithms have been proposed, such as [1], [12].

An independent quantization of the multiple channels would not be able to exploit the described azimuth oversampling. Considering the spectral selectivity offered by the present multi-channel system (as in Fig. 1), one easy way to get rid of such a sample correlation is, e.g., to perform a Fast Fourier Transform (FFT) before the data compression block. This allows for the implementation of an efficient quantization strategy, by allocating less resources for those sub-bands which "carry" a smaller amount of information, and vice-versa. In this scenario, a similar compression scheme for single-channel SAR has been proposed in [13].

Fig. 2 summarizes the workflow for the proposed strategy

Parameter	**Value**
Satellite Height, h_{sat}	700 km
Satellite Speed, v_{sat}	7500 m/s
Carrier Frequency, f_c	5.4 GHz
Pulse Repetition Frequency, PRF	1172 Hz
Total Processed Bandwidth, PBW	5600 Hz
Target Azimuth Resolution, Δ_{az}	1.2 m
Radar Wavelength, λ	5.55 cm
Azimuth Antenna Length, L_{az}	12.8 m
Number of Azimuth Channels, N	8
ADC Resolution	10 bits

Table 1: List of simulation parameters.

for onboard data reduction: for each instant of time m, the signal received by the i-th azimuth channel s_i ($\boldsymbol{s} \in \mathbf{R}^N$) is first digitized by an analog-to-digital converter (ADC) and then decomposed by means of an orthogonal transformation $\boldsymbol{M}$ ($\boldsymbol{M} \in \mathbf{R}^{K \times N}$). In our case, $\boldsymbol{M}$ corresponds to the digital Fourier transformation matrix (a more general transformation can be also considered). Then, a proper selection of the quantization rates is applied to the output transformed coefficients $\boldsymbol{y} = \boldsymbol{M}\boldsymbol{s}$ ($\boldsymbol{y} \in \mathbf{R}^K$), which are further compressed by means of a set of block adaptive quantizers (BAQ) [15] [16], represented by the BAQ b_i blocks (b_i expressed in bits/sample), in order to optimize the resulting data volume and performance. The set of quantized coefficients $\hat{\boldsymbol{y}}$ is then downloaded to the ground, where the inverse transform, multi-channel reconstruction [1], and signal focusing are carried out. In the following, we will refer to the present method as Multi-Channel Block Adaptive Quantization (MC-BAQ). Without loss of generality, we assume the number of output coefficients to be equal to the number of the input samples (i.e. $K = N$, for $K < N$ it is not strictly an orthonormal transform). Hence, for each instant of time m, the input signal array is decomposed into a set of K azimuth beams, each one corresponding to a different portion of the Doppler spectrum

$$y_k[\mathrm{m}] = \sum_{i=1}^{N} \left(s_{\mathrm{ADC},i}[\mathrm{m}]\right) e^{-j2\pi ik/N} \; k = [1, 2, ..., K]. \tag{3}$$

In the above relation, the same notation as in Fig. 2 has been used. The optimum bitrate to be selected for the k-th output channel is determined from rate-distortion theory [14] as

$$R_k = \bar{R} + \frac{1}{2}\log_2 \frac{{\sigma^2}_k}{\left[\prod_{l=1}^{K} {\sigma^2}_l\right]^{1/K}}, \tag{4}$$

where $\bar{R}$ is the mean allowable rate and ${\sigma^2}_k$ is the power associated to the k-th subband. In turn, this contribution is obtained as the fraction of the corresponding power

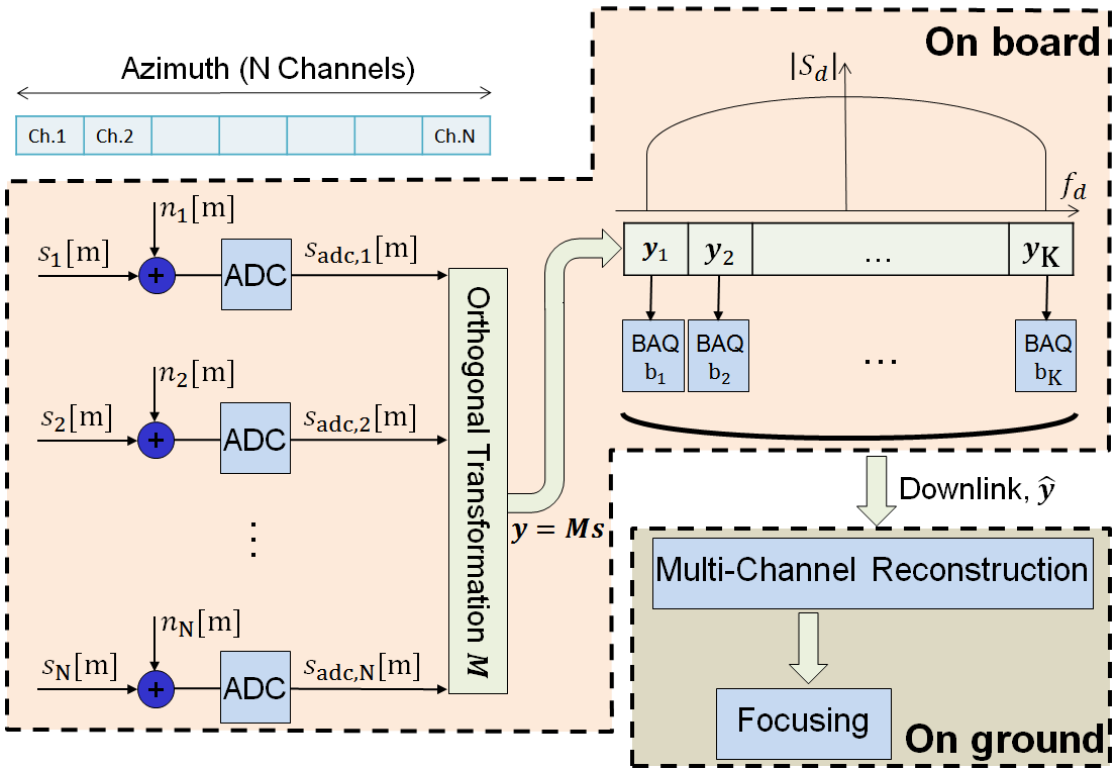

Figure 2: Workflow for the proposed MC-BAQ for onboard data reduction of a multi-channel SAR system: for each time instant m the signal received by the i-th azimuth channel, s_i, is first digitized by a high-precision analog-to-digital converter (10-bit ADC), and then decomposed by means of an orthogonal transformation M. As a next step, a proper selection of the quantization rates is applied to the transformed coefficients which are then compressed through a set block adaptive quantizers (the BAQ b_i blocks in the figure) to optimize the resulting data volume and performance. The quantized coefficients are then downloaded to the ground, where the inverse transform, multi-channel reconstruction, and signal focusing are carried out.

spectrum integrated over the output Doppler bandwidth

$$\sigma^2{}_k = \frac{\mathbf{E}_k}{K^2} \int_{-\mathrm{PBW}/2}^{\mathrm{PBW}/2} \left| \frac{\sin\left(\pi K \frac{f+\mathrm{PRF}(K/2-k)/K}{\mathrm{PRF}}\right)}{\sin\left(\pi \frac{f+\mathrm{PRF}(K/2-k)/K}{\mathrm{PRF}}\right)} \right|^2 . \tag{5}$$

Aside from of a normalization factor $1/K^2$, $\sigma^2{}_k$ is related to the energy associated to the k-th transformed coefficient $\mathbf{E}_k$, scaled by the integral of the Discrete Fourier Transform (DFT) kernel function over the processed bandwidth PBW, which is given by the relation

$$\sum_{k=0}^{N-1} e^{jkx} = e^{j(N-1)x/2} \frac{\sin(Nx/2)}{\sin(x/2)}. \tag{6}$$

The energy associated to the k-th transformed coefficient $\mathbf{E}_k$ represents the contribution of the antenna pattern in the corresponding portion of the Doppler spectrum, and is (offline) numerically estimated from a sequence of coefficients of length L as

$$\mathbf{E}_k = \sum_{m=0}^{L} |y_k[m]|^2. \tag{7}$$

Fig. 3 shows the Doppler power spectrum for the antenna

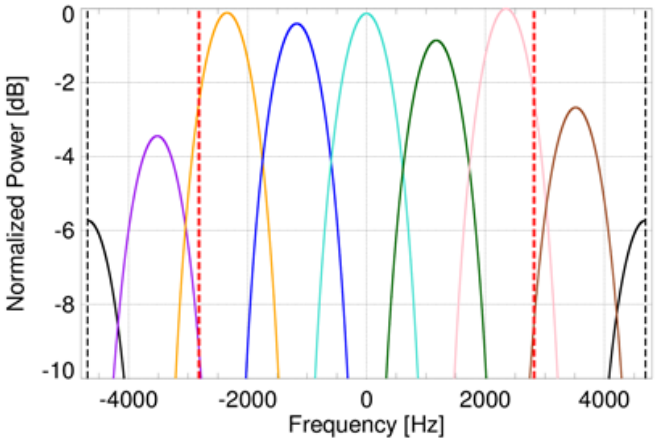

Figure 3: Doppler power spectrum for the eight azimuth channels, depicted with different colors. The resulting compression rate to be assigned to each channel is derived from (4), where the power term $\sigma^2{}_k$ is obtained by integrating the corresponding power spectrum in the range between -PBW/2 and PBW/2 (indicated by the dashed red lines), according to (5). The black dashed lines delimit the PRF interval.

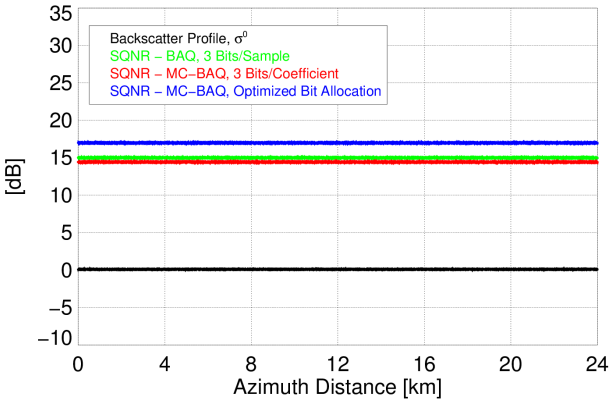

Figure 4: Backscatter profile and signal-to-quantization noise ratio (SQNR) for a distributed target. A mean rate of 3 bits/sample has been considered. Nominal BAQ with equal number of bits for each sample is depicted by the green line. Results from quantization in the Fourier domain, in case a constant BAQ rate for each sub-band is used, is shown by the red line. Finally, MC-BAQ with optimized bit allocation (according to (4) and rounded as in (10)) is depicted in blue.

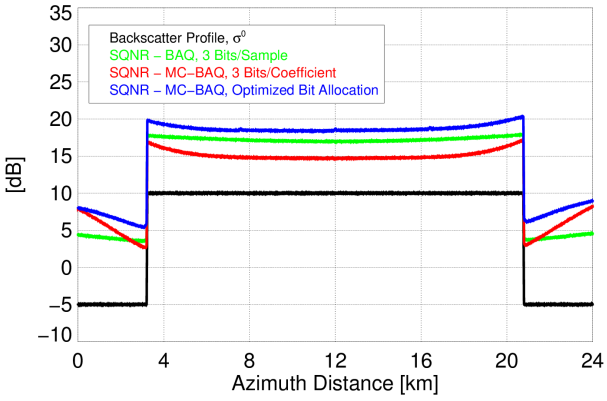

Figure 5: Backscatter profile and signal-to-quantization noise ratio (SQNR) for an artificial scene with a backscatter "jump" of 15 dB across the azimuth direction. A mean rate of 3 bits/sample has been considered. Nominal BAQ (i.e. operating independently on each channel) with equal number of bits for each sample is depicted by the green line. Results from quantization in the Fourier domain, in case a constant BAQ rate for each sub-band is used, is shown by the red line. Finally, MC-BAQ with optimized bit allocation (according to (4) and rounded as in (10)) is depicted in blue, and a performance improvement up to 3 dB is observed.

pattern displayed in Fig. 1 for the eight azimuth channels, each one depicted with a different color. The PRF and the PBW intervals are delimited by the dashed black and red lines, respectively.

In terms of onboard processing effort, for the implementation of a N=8 samples FFT, a modest amount in the order of a few tens of additional operations is required for each received range sample (exploiting the well known relation for the complexity $C = \mathcal{O}(n \log 2n)$).

3 Preliminary Results and Discussion

A first assessment of the proposed MC-BAQ method has been carried out for two simulated SAR scenes: a distributed target, showing a constant power distribution, and an artificial scene with a rectangular profile in azimuth direction. The corresponding azimuth profiles are sketched in black in Figs. 4 and 5, respectively. For the artificial scene, the backscatter step difference is of 15 dB, which represents a large dynamic range typically occurring in, e.g., urban area scenarios. For both scenes we have evaluated the signal-to-quantization noise ratio (SQNR), defined as the energy ratio of the uncompressed signal s to the quantization error ϵ affecting the reconstructed signal $\hat{s}$, $\epsilon = s - \hat{s}$

$$\mathrm{SQNR} = \frac{\sum_{p=1}^{P} |s_p|^2}{\sum_{p=1}^{P} |\epsilon_p|^2}, \tag{8}$$

being P the total number of pixels. The SQNR has been derived for different quantization strategies, which are shown in Figs. 4 and 5 with different colors. The green lines represent the "nominal" compression scheme, i.e. when each input sample is quantized (independently for each channel) with a constant BAQ rate at 3 bits/sample. The red lines, on the other hand, show the performance for quantization of the transformed Fourier coefficients with a constant compression rate for each coefficient (3-bit BAQ in this case). For this, the SQNR gets slightly worse (around 1-2 dB) if compared to the same bitrate allocation strategy independently for each channel. Finally, transform coding with optimized bit allocation (according to (4)) is shown by the blue lines, and a performance improvement up to 3 dB can be noticed, which verifies the potentials of the proposed method. For the artificial scene case in Fig. 5, a sensitive loss in terms of SQNR is observed for all compression techniques in the low backscatter area (with a mean backscatter of -5 dB) as a consequence of the "masking" effect induced by the presence of the high backscatter targets in close vicinity (this effect is usually referred to as low scatterer suppression [16], [17]). For the present example, considering the antenna pattern in Fig. 1 and the system parameters in Table 1, the set of compression rates $\boldsymbol{R}$ for 3 bits/sample is given in the following

$$\boldsymbol{R}_{3\mathrm{bits}} = \big[1.1, 1.8, 3.8, 3.8, 3.9, 3.8, 3.8, 1.9\big]. \tag{9}$$

However, it has to be pointed out, that the relation in (4) is strictly valid in case that the quantization errors are uniformly distributed and for large rates, which is not the case for typical SAR signal statistics and acquisition scenarios. Hence, one can conclude that the relation in (4) can be used as a starting reference for the bitrate selection, but then a numerical optimization of the bitrates may be needed. Possible benefits or performance improve-

ment in this context will be further investigated. For the specific example in Fig. 4 and 5 we have then rounded the bitrate set in (9) as follows

$$\boldsymbol{R}_{3\text{bits}} = \big[0, 2, 4, 4, 4, 4, 4, 2\big]. \tag{10}$$

It is worth pointing out that, even if the used sequence is not the optimum one, we still obtain a consistent performance improvement in terms of SQNR (lines blue vs lines green in Fig. 4 and 5). However, the resulting R_k are typically non-integer numbers. Instead of performing a rounding of the quantization rates, or embedding the quantizer with additional hardware/software blocks, fractional quantization rates can be "synthesized" by opportunely toggling the bitrate selection of an integer-bit quantizer along azimuth, as discussed in [18]. This way, higher flexibility of compression is achieved without increasing the overall scheme complexity. This aspect will be investigated in future studies.

4 Conclusions

In this paper on-board data volume reduction for multichannel synthetic aperture radar (SAR) systems is addressed. In this context, an increased amount of data is typically acquired in order to enlarge the unambiguous Doppler spectrum to be reconstructed on ground. Indeed, the samples received by the multichannel SAR instrument intrinsically exhibit some degree of correlation, which can be exploited to reduce the total amount of data to be stored and transmitted to the ground. For this purpose, an orthogonal transformation (FFT) is applied to the multichannel data, and, jointly, an efficient selection of the quantization rates is applied to the transformed radar data. Preliminary simulations are carried out for a single-platform C-band system, and for different SAR backscatter distributions, showing that the introduced Multi-Channel BAQ (MC-BAQ) grants a performance improvement (in the order of about 3 dB in SQNR for the considered examples), a gain which could also be exploited to achieve, for a given allowed distortion, a reduction of the resulting data volume.

References

[1] G. Krieger, N. Gebert, and A. Moreira *Unambiguous SAR signal reconstruction from non-uniform displaced phase center sampling*, IEEE Geosci. and Remote Sens. Lett., Vol. 1, no. 4, pp. 260-264, October 2004.

[2] N. Gebert, G. Krieger, and A. Moreira *Digital beamforming on receive: Techniques and optimization strategies for high-resolution wide-swath SAR imaging*, IEEE Trans. Aerosp. Electron. Syst., Vol. 45, no. 2, pp. 564-592, Apr. 2009.

[3] N. Gebert, M. Villano, G. Krieger, and A. Moreira *Errata: Digital Beamforming on Receive: Techniques and Optimization Strategies for High-Resolution Wide-Swath SAR Imaging*, IEEE Trans. Aerosp. Electron. Syst., Vol. 49, no. 3, p. 2110, July. 2013.

[4] M. Süss, and W. Wiesbeck *Side looking SAR system*, US Patent, US6870500B2, 22 March 2005.

[5] N. Gebert, G. Krieger, and A. Moreira *Multichannel azimuth processing in ScanSAR and TOPS mode operation*, IEEE Trans. Geosci. and Remote Sens., Vol. 48, no. 7, pp. 2994-3008, July 2010.

[6] N. Gebert, M. Villano, G. Krieger, and A. Moreira *Correction to Multichannel Azimuth Processing in ScanSAR and TOPS mode operation*, IEEE Trans. Geosci. and Remote Sens., Vol. 51, no. 8, pp. 4611, July 2013.

[7] N. Gebert, G. Krieger, and A. Moreira *SAR signal reconstruction from non-uniform displace phase center sampling in presence of perturbation*, IEEE Int. Geosci. Remote Sens. Symp., Seoul (South Korea), November 2005.

[8] P. Guccione, M. Scagliola, and D. Giudici *Principal Components Dynamic Block Quantization for multichannel SAR*, IEEE Int. Geosci. Remote Sens. Symp., pp. 1034-1037, Bejing (China), July 2016.

[9] E. Attema, C. Cafforio, M. Gottwald, P. Guccione, A. M. Guarnieri, F. Rocca, and P. Snoeij, *Flexible Dynamic Block Adaptive Quantization for Sentinel-1 SAR Missions*, IEEE Geosci. and Remote Sens. Lett., Vol. 7, no. 4, pp. 766-770, October 2010.

[10] S. Barbarossa, *Detection and imaging of moving objects with synthetic aperture radar. Part 1. Optimal detection and parameter estimation theory.*, IEE Proceedings - F (Radar Signal Processing), vol. 139, no. 1, pp. 79-88, January 1992.

[11] M. Villano, G. Krieger, and A. Moreira *Advanced Spaceborne SAR Systems with Planar Antenna*, IEEE Radar Conference, Seattle, WA, USA, May 2017.

[12] D. Cerutti-Maori, I. Sikaneta, J. Klare, and C. H. Gierull *MIMO SAR Processing for Multichannel High-Resolution Wide-Swath Radars*, IEEE Trans. Geosci. and Remote Sens., Vol. 52, no. 8, pp. 5034-5055, August 2014.

[13] J. Fisher, U. Benz, and A. Moreira, *Efficient SAR raw data compression in frequency domain*, IEEE Int. Geosci. Remote Sens. Symp., pp. 1034-1037, Hamburg (Germany), July 1999.

[14] N. S. Jayant, and P. Noll, *Digital Coding of Waveforms*, Prentice Hall, 1984.

[15] R. Kwok, and W. Johnson, *Block Adaptive Quantization of Magellan SAR Data*, IEEE Trans. on Geosci. and Remote Sens., Vol. 27, no. 4, pp. 375-383, August 1989.

[16] M. Martone, B. Bräutigam, and G. Krieger, *Quantization effects in TanDEM-X data*, IEEE Trans. on Geosci. and Remote Sens., Vol. 53, no. 2, pp. 583-597, February 2015.

[17] S. Huber, M. Younis, and G. Krieger, *The TanDEM-X mission: overview and interferometric performance*, Int. J. Microw. Wireless Technol., vol. 2, no. 3/4, pp. 379-389, July 2010.

[18] M. Martone, B. Bräutigam, and G. Krieger, *Azimuth Switched Quantization for SAR systems and performance analysis on TanDEM-X data*, IEEE Geosci. and Remote Sens. Lett., Vol. 11, no. 1, pp. 181-185, January 2014.